Odontology (2024) 112:341–354
https://doi.org/10.1007/s10266-023-00836-7

ORIGINAL ARTICLE

Evaluation of the antibacterial activity of dental adhesive containing biogenic silver nanoparticles decorated nanographene oxide nanocomposites (Ag@nGO NCs) and effect on bond strength to dentine

Soley Arslan[1] · Semiha Ekrikaya[2] · Nilay Ildiz[3] · Sadi Yusufbeyoglu[4] · İsmail Ocsoy[5]

Received: 5 April 2023 / Accepted: 30 June 2023 / Published online: 12 July 2023
© The Author(s), under exclusive licence to The Society of The Nippon Dental University 2023

Abstract

Our study aimed to evaluate the antibacterial activities and dentin bond strengths of silver nanoparticles (Ag NPs) and silver nano-graphene oxide nanocomposites (Ag@nGO NCs) produced by green and chemical synthesis methods added to the dental adhesive. Ag NPs were produced by green synthesis (biogenic) (B-Ag NPs) and chemical synthesis methods (C–Ag NPs) and deposited on nGO (nano-graphene oxide). Ag NPs and Ag@nGO NCs (0.05% w/w) were added to the primer and bond (Clearfil SE Bond). Group 1: control, Group 2: nGO, Group 3: B-Ag NPs, Group 4: B-Ag@nGO NCs, Group 5: C–Ag NPs, Group 6: C–Ag@nGO NCs. *Streptococcus mutans (S. mutans)* live/dead assay analysis, MTT metabolic activity test, agar disc diffusion test, lactic acid production, and colony forming units (CFUs) tests were performed. Bond strength values were determined by the microtensile bond strength test (μTBS). Failure types were determined by evaluating with SEM. Statistical analysis was performed using one-way ANOVA and two-way ANOVA ($p < 0.05$). There was a difference between the groups in the viable bacteria ratio and lactic acid production tests ($p < 0.05$). When the inhibition zone and *S. mutans* CFUs were evaluated, there was no difference between Group 3 and Group 4 ($p > 0.05$), but there was a difference between the other groups ($p < 0.05$). When the metabolic activity of *S. mutans* was evaluated, there was a difference between Group 1 and other groups, and between Group 2 and Group 5, and Group 6 ($p < 0.05$). There was no difference between the groups in the μTBS values ($p > 0.05$). As a result, although the antibacterial activity of B-Ag NPs and B-Ag@nGO Ag NPs obtained by green synthesis is lower than that of chemically synthesis obtained C–Ag NPs and C–Ag@nGO NCs, they provided higher antibacterial activity compared to the control group and did not reduce μTBS. The addition of biogenic Ag NPs to the adhesive system increased the antibacterial effect by maintaining the bond strength of the adhesive. Antibacterial adhesives can increase the restoration life by protecting the tooth-adhesive interface.

Keywords Antibacterial activity · Biogenic Ag NPs · Biogenic Ag@nGO NCs · Bond strength · Dental adhesive

Soley Arslan and Semiha Ekrikaya contributed equally to this work.

✉ Semiha Ekrikaya
semihaekrikaya@gmail.com

Soley Arslan
soley@erciyes.edu.tr

Nilay Ildiz
nilaygucluer@yahoo.com

Sadi Yusufbeyoglu
sd.ysfbygl@gmail.com

İsmail Ocsoy
ismailocsoy@erciyes.edu.tr

[1] Department of Restorative Dentistry, Faculty of Dentistry, Erciyes University, Kayseri, Turkey

[2] Department of Restorative Dentistry, Faculty of Dentistry, Nuh Naci Yazgan University, Kayseri, Turkey

[3] Department of Pharmaceutical Microbiology, Faculty of Pharmacy, Erciyes University, Kayseri, Turkey

[4] Department of Pharmaceutical Botany, Faculty of Gulhane Pharmacy, University of Health Sciences, Ankara, Turkey

[5] Department of Analytical Chemistry, Faculty of Pharmacy, Erciyes University, Kayseri, Turkey

Introduction

The ecological plaque hypothesis argues that dental caries occur due to dysbiosis in the balance of oral microflora. The main mechanism of caries formation is demineralization by fermentable carbohydrates and acids produced by bacteria in dental plaque biofilms. After dental caries have occurred, the treatment procedure involves removing the decayed dental tissues and filling the cavity with restorative material [1].

In restorative treatments, while the caries tissue is cleaned, residual bacteria may remain in the cavity. In addition, microleakage and bacterial infiltration can be seen in restorative treatments due to adhesive failures and microgaps [2]. Antibacterial dental materials can be used to combat bacteria that can cause secondary caries. The antibacterial properties of dental adhesives can provide an important advantage for restoration success. Therefore, studies are carried out to develop dental adhesives using NPs [3–5]. NPs are classified into organic, inorganic, and carbon-based types. Organic NPs are known to be non-toxic, and biologically degradable. On the other hand, inorganic NPs, which do not consume carbon during their synthesis, include metal and metal oxide NPs [6]. For the antibacterial effect, studies were conducted using chlorhexidine gluconate, sodium hypochlorite, hydrogen peroxide, iodine, benzalkonium chloride, ozone gas, and lasers in dental materials. Additionally, monomers such as MDPB, DMAE-CB, DMADDM, QADM, fluorine, and metal ions such as Cu^{2+}, Zn^{2+}, Ag^{+} have been added to dental adhesives for antibacterial effect [3–5].

The potential antimicrobial mechanisms of silver nanoparticles (Ag NPs) are explained by the ability of Ag^{+} ions to inhibit bacterial enzymes or inactivate the DNA replication ability of bacteria [7–9]. Previous studies have reported that Ag NPs have high antibacterial activities in dental materials [10–13]. Studies have shown that Ag NPs have a potent antibacterial activity that greatly reduces biofilm growth and lactic acid production without adversely affecting the physical and mechanical properties of dental resins [14–16].

Recently, biogenic Ag NPs have been actively synthesized by the green synthesis method, using various biomolecules including plant extracts, enzymes, and DNA [17–27]. Different types of plant extracts were used to synthesize Ag NPs. Plant-mediated biosynthesis of NPs in green tea (*Camelia sinensis*) chamomile (*Matricaria chamomilla*), black pepper (*Piper nigrum*), lavender (*Lavandula officinalis*), sage (*Salvia officinalis*), clove (*Syzygium aromaticum*), rosemary (*Rosmarinus officinalis*), thyme (*Thymus vulgaris*), and laurel (*Laurus nobilis*) are used [28]. In current studies, biogenic NPs synthesized by the green synthesis method attract more attention than chemically synthesized NPs [19, 20]. In chemical methods, toxic reducing and stabilizing agents are generally used for the synthesis of NPs. Toxicity is the main disadvantage in biological application. Therefore, there is a need for non-toxic synthesis methods. In this regard, the green synthesis method provides a significant advantage [25, 27]. However, the main disadvantages of DNA, proteins, or enzymes are their high cost, low stability, and easy contamination. Therefore, it is recommended to use plant extracts in the synthesis of biogenic NPs. The advantages of plants can be listed as quite cost-effectiveness, easy availability, less contamination risk, and high stability. [19–27].

In current studies in dentistry, GO (graphene oxide) application has been used successfully in Antibacterial effect, regenerative dentistry, bone tissue engineering, drug delivery, increasing the physicomechanical properties of dental biomaterials, implant surface modification, and oral cancer treatment. Due to the biocompatibility of graphene oxide and nanocomposites, it can be used successfully in bone regeneration, osseointegration, and cell proliferation. Additionally, due to its antibiofilm properties, the use of GO for biofilm and caries prevention is becoming widespread [29, 30]. GO is used as a platform to hold the NPs on their surface and prevent their aggregation. The reported studies have shown that Ag NPs deposited on the GO surface have a greater antibacterial activity compared to bare Ag NPs and GO [29–32].

In our study, biogenic Ag NPs and Ag@nGO nanocomposites (NCs) produced with chamomile plant extracts were added to increase the antibacterial effectiveness of dental adhesives. Chamomile extract acted as a reducing and stabilizing agent owing to the rich phenolic compounds, for the synthesis of Ag NPs. Chamomile plants were also preferred because it does not cause a color change and it possesses a mild antibacterial activity. Additionally, chemically reduced Ag NPs were used in all adhesive studies reported in the literature [2, 29–33].

The aim of clinical applications is to provide cavity disinfection and create long-lasting restorations. Therefore, efforts are being made to develop adhesives containing antibacterial nanoparticles. However, there is a lack of sufficient studies on this topic in the literature. Existing studies primarily involve nanoparticles produced using chemical methods. Furthermore, there is no study utilizing graphene oxide (GO) in dental adhesives. In our study, chemically synthesized Ag NPs and Ag@nGO NCs (referred to as C–Ag NPs and C–Ag@nGO NCs) as well as Ag NPs and Ag@nGO NCs produced using green synthesis (biogenic) methods (referred to as B-Ag NPs and B-Ag@nGO NCs) were employed. We have pioneered the use of green synthesis methods for the synthesis of both Ag NPs and Ag@nGO

NCs and their incorporation into dental adhesives. Additionally, our study aimed to enhance the antibacterial activities of dental adhesives and preserve dentin bond strengths by utilizing Ag NPs and Ag@nGO NCs. The null hypothesis of this study "Dental adhesive group containing B-Ag@nGO NCs will provide higher antibacterial activity in dental adhesive groups containing B-Ag NPs, C–Ag NPs, C–Ag@nGO NCs and will not decrease bond strength to dentin" is in the form.

Materials and methods

This study protocol was approved by the Erciyes University Faculty of Medicine Ethics Committee (2020\519).

Preparation of the chamomile extract

To obtain chamomile extract, chamomile was firstly cleaned, weighed at a certain rate, mixed with 100 mL of deionized water, and boiled for 5 min. The mixture was then cooled to room temperature (20 ℃) and filtered through Whatman filter paper. The obtained extract was stored in a closed container in a refrigerator at + 4 ℃ to be used for both total phenol determination and Ag NP synthesis. The extract was used as a reducing and stabilizing agent in Ag NPs synthesis.

Synthesis of Ag NPs using chamomile extract

As a general synthesis procedure, a certain amount of chamomile extract (5 mL of 5%) was added to the silver nitrate (1 mM 50 mL) solution and incubated with the final mixture at 85 ℃ for 40 min under a magnetic stirrer. After incubation, the color change was observed in the mixture, it was cooled to room temperature and centrifuged at 10,000 rpm. Centrifugation was repeated 2 times. The excess plant extract was removed with the supernatant and Ag NPs solutions were saved for characterization and application. The absorbance spectra of Ag NPs and plant extract aqueous solutions were measured using a UV–Vis spectrophotometer. The morphology of Ag NPs was visualized by scanning electron microscopy (SEM) (LEO-440, Zeiss, Cambridge, England). Energy-dispersive X-ray (EDX) spectroscopy was used for the elemental analysis of Ag NPs. The presence of plant extracts on the surface of Ag NPs was confirmed by FT-IR spectrometry.

Synthesis of Ag@nGO NCs

GO synthesis was performed using a modified Hummers method [19]. NaCl solution at different concentrations was added in two steps to bond Ag NPs to the nGO surface. While nGO (0.1 mg/mL) was mixed, the previously synthesized Ag NPs solution was added. While stirring continued, the first NaCl solution (2.4 mL, 0.09 M) was added dropwise, followed by the second NaCl solution (5 mL, 0.29 M). The mixture was centrifuged at 3000 rpm for 5 min. Thus, Ag NP@GO NCs were separated by centrifugation. Ag@nGO NCs were dispersed in 5 mL of deionized water and it was centrifuged thrice [32].

Characterization of Ag NPs, nGO, and Ag@nGO NCs

STEM was used to characterize the morphology of Ag NPs, nGO, and Ag@nGO NCs. The characteristic absorbance points of Ag NPs, nGO, and Ag@nGO NCs were determined by UV–Vis spectrophotometer. The presence and ratio of Ag in Ag@nGO NCs were determined using Energy-dispersive X-ray spectrometry.

Study groups

Antibacterial activity was assessed by incorporating Ag NPs into dental adhesives (Clearfil SE Bond, Kuraray, Okayama, Japan) at different weight ratios (0.25%, 0.05%, 0.1%). Because of Antibacterial tests, the optimum effect was determined at 0.05% by weight Ag NPs concentration. For this reason, 0.05% by weight Ag NPs were added to both the primary and bond components of the dental adhesive. The NP ratio was determined similarly in other groups.

Group 1: Primer + Bond (Control group)

Group 2: Primer + 0.05% nGO, Bond + 0.05% nGO

Group 3: Primer + 0.05% B-Ag NPs, Bond + 0.05% B-Ag NPs

Group 4: Primer + 0.05% B-Ag@nGO NCs, Bond + 0.05% B-Ag@nGONCs

Group 5: Primer + 0.05% C–Ag NPs, Bond + 0.05% C–Ag NPs

Group 6: Primer + 0.05% C–Ag@nGO NCs, Bond + 0.05% C–Ag@nGO NCs

Calculation of the sample size

The sample size for our study was estimated using data from a previous similar study [33]. Using the G-Power application, the sample size for the microtensile bond strength (μTBS) test was determined to be 16 at a significance level of $\alpha = 0.05$ and a power $(1 - \beta)$ of 0.95, to a 95% confidence level. To account for the expected losses, 20% was added to the calculated study group, and 20 samples were included in each group. Two dentin-composite rods were obtained from each tooth sample. A total of 60 human third molars were used for 6 groups.

Preparation of resin specimens for antibacterial tests

A silicone mold with a diameter of 10 mm and a height of 2 mm was used to prepare the sample. 10 µl of primer were placed on the bottom of the mold and 10 s air dried. Then, 10 µl of the bond were added, 10-s air dried, and photopolymerized (VALO LED, Ultradent, South Jordan, UT, USA) for 20 s. Afterward, the composite resin (Z550 XT, 3 M ESPE, St. Paul, MN, ABD) was placed and pressed with a glass plate on the silicone mold and polymerized for 60 s. With this method, a three-layer primer/bond/composite disc with a diameter of about 10 mm and a thickness of 2 mm was obtained. Prepared samples were kept in deionized water at 37 ℃ for 24 h for post-polymerization. The discs were then sterilized with ethylene oxide. The composite surface of the resin discs was marked with a pencil and the adhesive surface was used for antibacterial tests. For *Streptococcus mutans (S. mutans)* live/dead assay analysis, MTT metabolic activity test, agar disc diffusion test, lactic acid production, and CFUs values, 3 discs discs each group were used for each test.

Antibacterial tests

Biofilm-forming *S. mutans* ATCC 25175 was used in our antibacterial studies. Subculture was obtained by incubating the bacteria in tryptic soy broth containing 1% sucrose anaerobically for 24 h at 37 ℃. To create a 24-h *S. mutans* biofilm, resin disc samples were placed in a 24-well plate with the adhesive on top. The saliva-glycerol stock was added to 2-ml BHI or McBain at a 1:50 dilution. 1.5-mL inoculum was added to each well and incubated in 5% CO_2 at 37 ℃ for 8 h. The discs were then transferred to new 24-well plates and incubated again under the same conditions for 16 h. After 16 h, the discs were transferred to new 24-well plates and incubated for 24 h at 37 ℃ at 5% CO_2 [34].

Live/dead assay

Discs containing 24 h biofilm were washed with phosphate-buffered saline. Bacteria were stained using the live/dead bacteria kit. Syto 9 was used to produce a green fluorescence in live bacteria. Bacteria with poor membranes were stained with propidium iodide to produce a red fluorescence. Also, planktonic bacteria in the medium were similarly stained for live/dead discrimination. 3 samples were tested for each group ($n=3$). Stained samples were examined with a confocal laser microscope (Zeiss LSM 710, Carl Zeiss, Oberkochen Germany) [33, 35, 36].

S. mutans MTT metabolic activity

Discs containing 24 h biofilm were transferred to a 24-well plate with 1-mL MTT dye in each chamber. All samples were incubated at 37 ℃ in 5% CO_2 for 1 h. After 1 h, the biofilm samples were transferred to a new 24-well plate. Planktonic bacteria were collected by centrifugation. 1 mL of dimethyl sulfoxide was added to dissolve the formazone crystals. After 20 min of incubation in the dark, the absorbance at 540 nm of 200 L DMSO solution was measured with a microplate reader. 3 samples were tested for each group ($n=3$) [37, 38].

Agar disc diffusion test

Mueller Hinton agar was used as the medium. An agar borer (cork borer) was used to create a hole of the desired diameter (6 mm) in agar that was sterilized in an autoclave and poured into Petri dishes. Wells of the desired dimensions were opened with a sterilized agar drill. The suspension method was used to prepare the bacterial solution. For this purpose, 0.5 McFarland bacterial solution was prepared from 18 to 24 h of culture, and spread cultivation was performed on agar Petri dishes with a swab (EUCAST, 2019). Inhibition zones were measured after 24 h of incubation under anaerobic conditions. The study was performed in three replicates, and experiments were concluded with negative/positive controls.

Lactic acid production and colony-forming units (CFUs)

Discs containing 24 h biofilm were washed with cysteine peptone water (CPW) and placed in a 24-well plate. Planktonic bacteria were collected by centrifugation for 4 min. 1.5 mL of buffered peptone water (BPW) supplemented with 0.2 sucrose was added to each well. The samples were incubated for 3 h at 37 ℃ with 5% CO_2 to allow the bacteria to produce acid. After 3 h, the BPW solutions were stored for lactate analysis. Lactate concentrations were determined using the enzymatic method. A microplate reader was used to measure the absorbance of the collected BPW solutions at 340 nm. Bacteria in biofilms on discs ($n=3$) were harvested by sonication, and CFU numbers of planktonic bacteria in the medium were measured [37, 38].

Microtensile bond strength (µTBS) test

In our study, 60 non-carious extracted human third molar teeth from individuals aged 18–30 were used. The occlusal third of the dental crown was cut to expose the middle coronal dentine. The dentine surface was polished with 600–800-1000 grit SiC paper. The surface was washed and dried for 30 s.

Primer (Clearfil SE Bond, Kuraray, Okayama, Japan) was applied to the tooth surface, left for 20 s, and the solvent was removed by applying air for 5 s. Then, Bond (Clearfil SE Bond, Kuraray, Okayama, Japan) was applied, thinned with air for 10 s, and cured with light (VALO LED, Ultradent, South Jordan, UT, USA) for 10 s. Layered composite resin (Z550 XT, 3 M ESPE, St. Paul, MN, USA) was placed on the dentine surface with the help of matrix tape, and each layer was light-cured for 60 s. All the samples were kept in deionized water at 37 ℃ for 24 h to complete the polymerization. Sections were taken from each tooth to obtain two 1 mm × 1 mm wide and 8 mm long resin-dentin rods (Isomet 1000; Buehler, Lake Bluff, IL, USA). For each group, 10 teeth were used and 20 composite-dentine bars ($n = 20$) were created. The rods were broken under uniaxial tension at 1 mm/min on a computer-aided microtensile device (MTD-500 plus, Westerham, Germany). The fracture values were recorded in megapascals (MPa).

The surfaces of the samples were coated with gold and examined by SEM (LEO-440, Zeiss, Cambridge, England) to determine the failure modes (adhesive, cohesive, mixed). If a complete fracture occurs between different materials (eg, between the tooth tissue and the composite resin), it is defined as an adhesive type failure. If the fracture occurs within the material itself, it is defined as a cohesive type failure. The failure type in which adhesive and cohesive failures occur together is referred to as a mixed type failure [39].

Statistical analysis

Statistical analyzes were performed using GraphPad Prism version 8.0.1 software. One-way ANOVA test was used for statistical analysis of antibacterial tests. Kolmogorov–Smirnov analysis was used to test the distribution of the data. Two-way ANOVA was performed for comparison between groups in the μTBS. The Tukey post hoc test was used for mean comparison. Descriptive statistics were given as a number of units (n), percent (%), and mean ± standard deviation $\left(\bar{x} \pm ss\right)$. ($p < 0.05$) was considered statistically significant in all comparisons.

Results

Synthesis and characterization of nanoparticles

The morphologies of NPs, have been characterized using scanning transmission electron microscopy (STEM) images. C–Ag and B-Ag NPs have been shown to have highly smooth and spherical morphologies of approximately 15 nm in Figs. 1A and 2A, respectively. In addition that, the Ag NPs were homogeneously immobilized on the surface of GO oxide without certain agglomeration as seen in STEM images of both Figs. 1B and 2B.

The characteristic absorbance points of C–Ag NPs and C–Ag@nGO NCs in Fig. 1C, D and B-Ag NPs, B-Ag@nGO NCs in Fig. 2C, D were determined by UV–Vis spectrophotometer. While the characteristic absorption peaks of both C–Ag NPs and B-Ag NPs were observed between 420 and 440 nm (Figs. 1C and 2C), C–Ag@nGO NCs and B-Ag@nGO NCs have absorbance peaks between 450 and 480 nm (Figs. 1D and 2D) with approximately 35 nm shift due to small aggregation of the Ag NPs on GO and occurrence of the electron junction between Ag NPs and GO.

Additionally, the surface charges of C–Ag NPs and C–Ag@nGO NCs in Fig. 1E, F and B-Ag NPs, and B-Ag@nGO NCs in Fig. 2E, F were determined by zeta potential. In terms of surface charge, both the surface charge of C–Ag NPs and B-Ag NPs were determined by Zeta potential measurements to be around − 23 mV (Figs. 1E and 2E; however, zeta-potential values of C–Ag@nGO and B-Ag@nGO NCs gave negative surface charge with − 32 mV (Figs. 1F and 2F) owing to the presence of hydrophilic carboxy groups on GO.

EDX analysis

The Ag presence and ratio in B\C–Ag@nGO NCs were determined using energy-dispersive X-ray (EDX) spectrometry. Because of EDX analysis, Ag metal presence was detected due to B\C–Ag NPs added in primer, bond, and primer + bond. The weight percent ratios (w/w) in the Ag NPs primer and bond are shown in (Figs. 3 and 4). In addition to the EDX spectra because of the EDX analysis, the presence of Ag metal was demonstrated by EDX mapping (Figs. 3 and 4).

Antibacterial tests

Live bacteria, *S. mutans* MTT metabolic activity, agar disc diffusion, lactic acid production, and CFUs values of all groups are given in Table 1.

Live/dead assay

There was a statistically significant difference between the groups ($p < 0.05$). The lowest viability/live ratio of bacteria was in Group 6 (Fig. 5).

S. mutans MTT metabolic activity

There was a statistically significant difference between Group 1 and other groups, and between Group 2 and Group 5 and 6 ($p < 0.05$). There was no statistically significant difference between the other groups ($p > 0.05$) (Fig. 5).

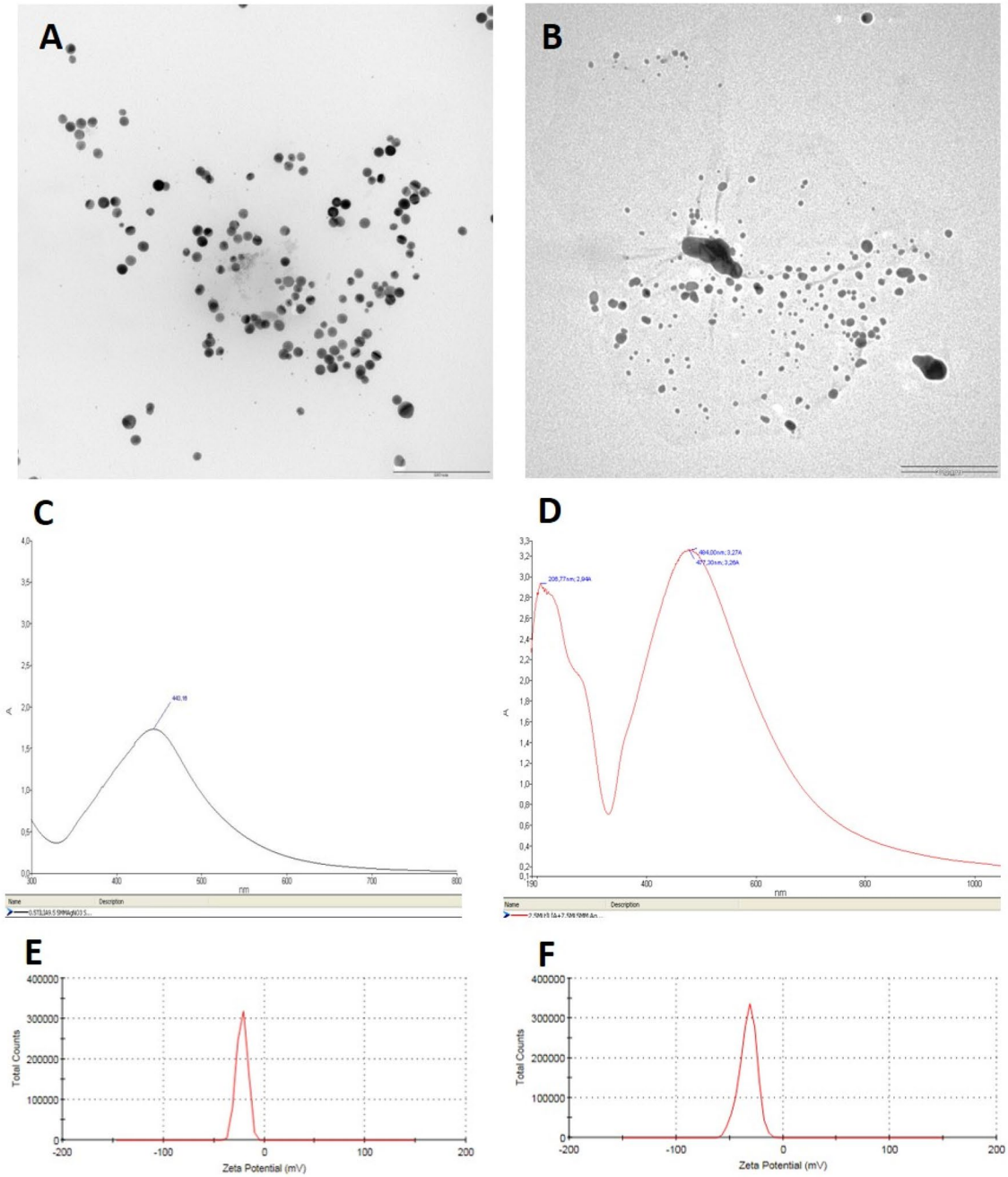

Fig. 1 STEM image of **A** C-Ag NPs **B** C-Ag@nGO NCs, UV–Vis spectrum of **C** C-Ag NPs and **D** C-Ag@nGO NCs, Zeta potential measurement of **E** C-Ag NPs and **F** C-Ag@nGO NCs. (*C-Ag NPs* Chemical silver nanoparticles, *C-Ag@nGO NCs* Chemical silver nano-graphene oxide nanocomposites)

Agar disk diffusion test

There was no statistically significant difference between Group 3 and Group 4 ($p > 0.05$). There was a statistically significant difference between the other groups ($p < 0.05$). The largest inhibition zone value in millimeters was observed in Group 6 (Fig. 5).

Lactic acid production

There was a statistically significant difference between all groups ($p < 0.05$). Lactic acid production was at least in Group 6 (Fig. 5).

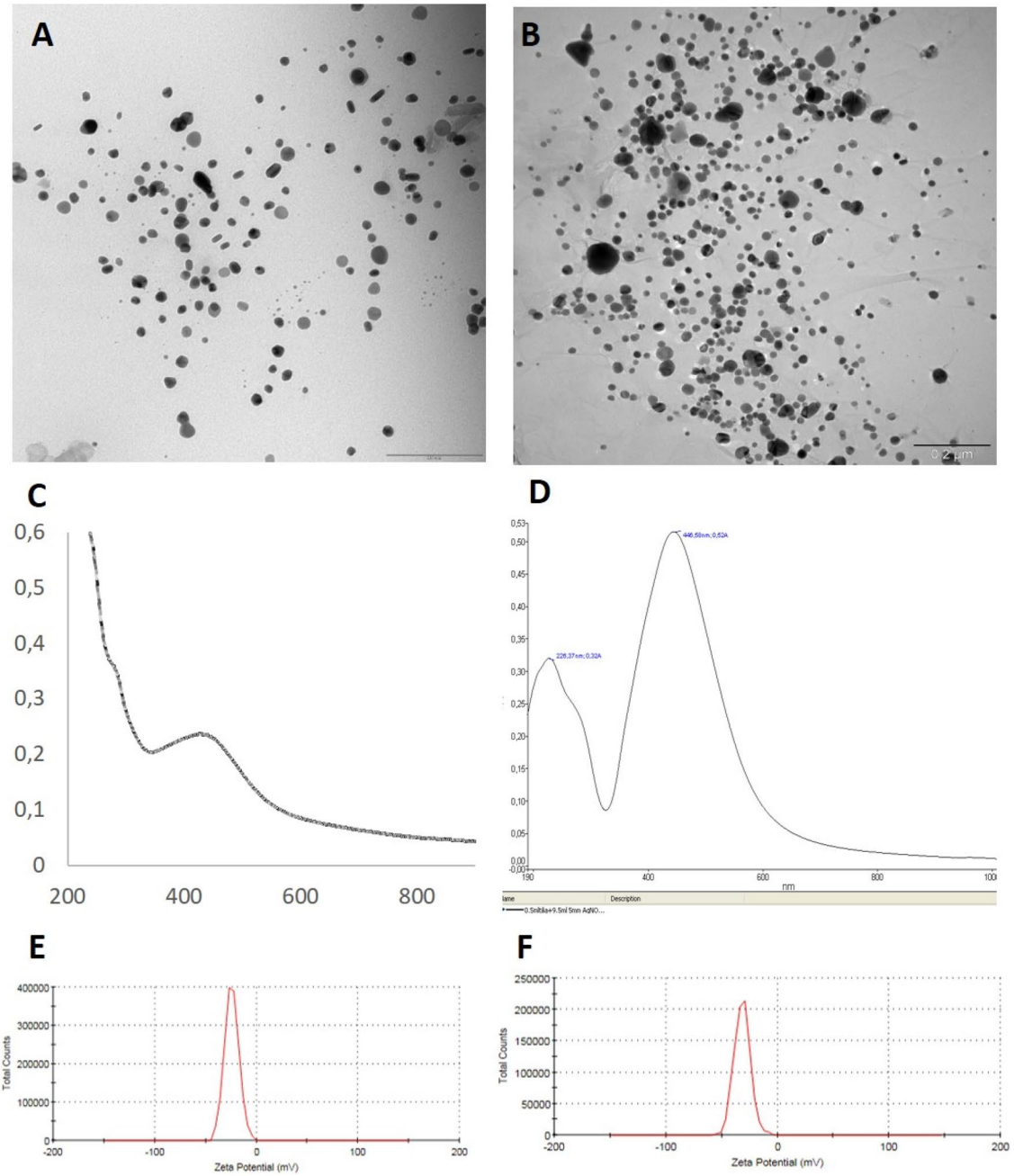

Fig. 2 SREM image of **A** B-Ag NPs **B** B-Ag@nGO NCs, UV–Vis spectrum of **C** B-Ag NP and **D** B-Ag@nGO NCs, Zeta potential of measurement of **E** B-Ag NPs and **F** B-Ag@nGO NCs. (*B-Ag NPs* Biogenic silver nanoparticles, *B-Ag@nGO NCs* Biogenic silver nanographene oxide nanocomposites)

S. mutans colony-forming units (CFUs)

There was no statistically significant difference between Group 3 and Group 4 ($p > 0.05$). There was a statistically significant difference between the other groups ($p < 0.05$). *S. mutans* colony-forming unit was seen at least in Group 6 (Fig. 6).

Microtensile bond strength test

In Table 2, the mean and standard deviations of the bond strength values of the groups in megapascals (Mpa) and the failure modes are given.

There was no statistically significant difference between the groups in terms of dentine bond strength ($p > 0.05$).

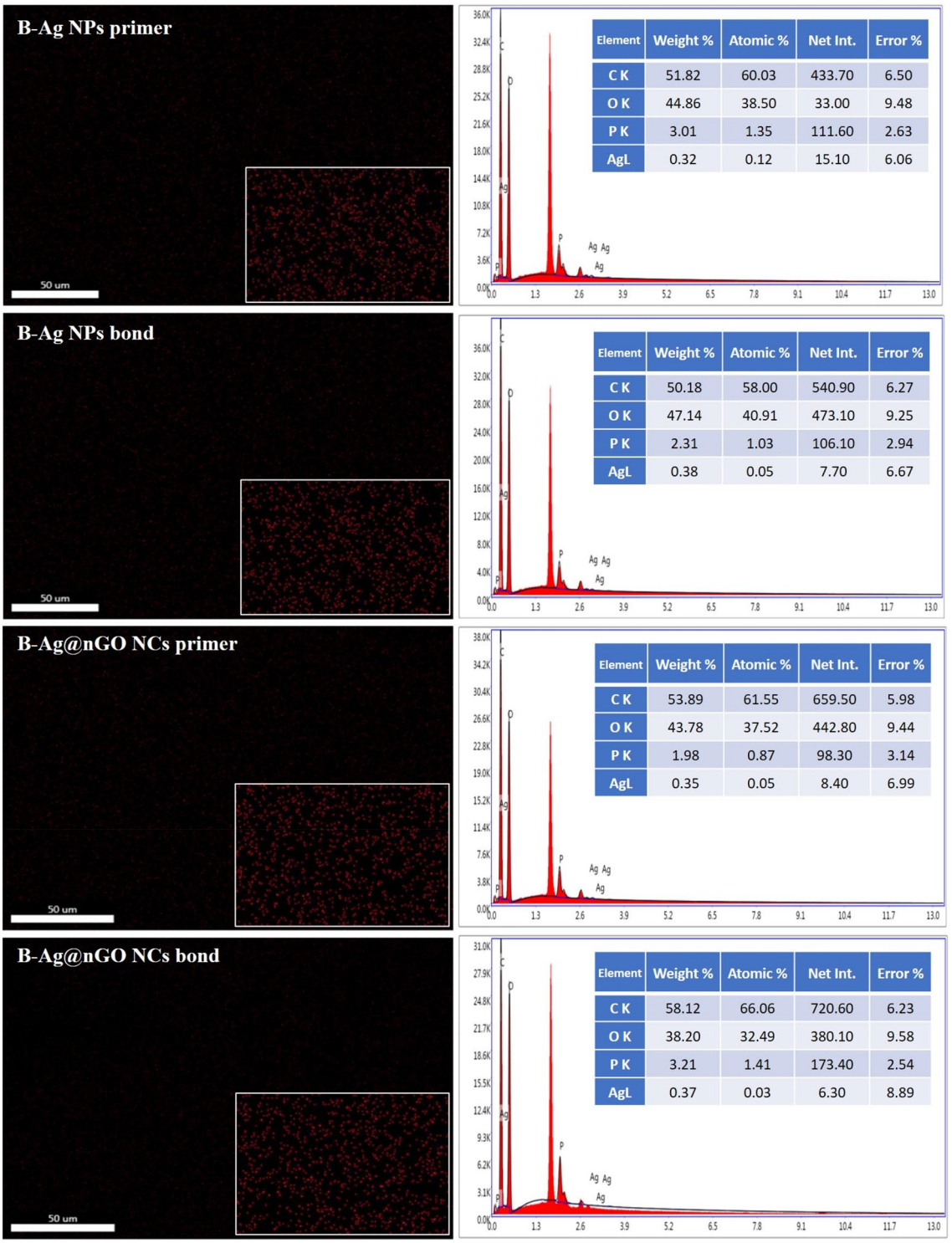

Fig. 3 EDX spectrum of primer and bond containing B-Ag NPs and B-Ag@nGO NCs and showing Ag metal. (*B-Ag NPs* Biogenic silver nanoparticles, *B-Ag@nGO NCs* Biogenic silver nano-graphene oxide nanocomposites)

When the failure modes were evaluated, the percentage of mixed failure modes was higher in Group 1 and Group 3 cohesive failure modes were more common in Group 5 and Group 6.

Discussion

The main purpose of our study was to evaluate the antibacterial activity and dentin bond strength of dental adhesives

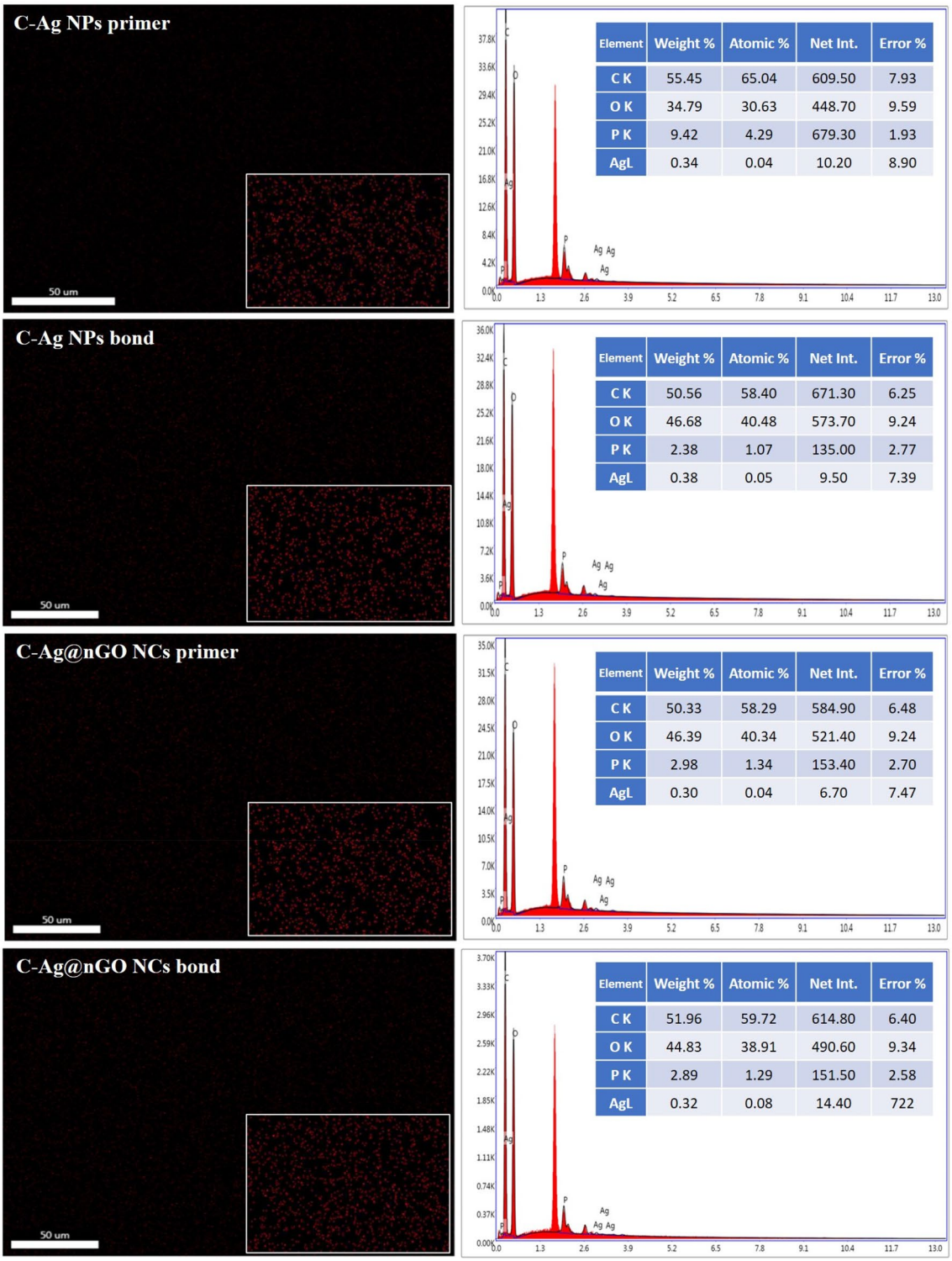

Fig. 4 EDX spectrum of primer and bond containing C-Ag NPs and C-Ag@nGO NCs and showing Ag metal. (*C-Ag NPs* Chemical silver nanoparticles, *C-Ag@nGO NCs* Chemical silver nano-graphene oxide nanocomposites)

containing B-Ag NPs, B-Ag@nGO NCs, C–Ag NPs, and C–Ag@nGO NCs. According to our study results, adhesive groups containing C–Ag@nGO NCs showed higher antibacterial activity than groups of B-Ag NPs and B-Ag@nGO NCs. There was no difference in dentin bond strength when the NPs added nanoparticle groups were compared

Table 1 Mean, standard deviation, and statistical differences of live bacteria, *S. mutans* MTT metabolic activity, agar disc diffusion, lactic acid production, and CFU values of the groups

Groups	Live bacteria (%)	*S. mutans* MTT activity (A_{540})	Agar disc diffusion (mm)	Lactic acid production (mmol/L)	CFU_s ($10^{6/disc}$)
Group 1 (Control)	96.48 (±0.685)[a]	0.495 (±0.495)[a]	8.057 (±0.141)[a]	12.06 (±0.084)[a]	21.61 (±0.304)[a]
Group 2 (nGO)	65.32 (±0.466)[b]	0.298 (±0.495)[b]	8.9 (±1.27)[b]	10.555 (±0.629)[b]	13.565 (±0.799)b
Group 3 (B-Ag NPs)	51.26 (±0.376)[c]	0.197 (±0.495)[bc]	17.08 (±0.113)[c]	6.25 (±0.353)[c]	7.85 (±0.212)[c]
Group 4 (B-Ag@nGO NCs)	47.23 (±0.325)[d]	0.188 (±0.840)[bc]	20.095 (±0.134)[c]	5.2 (±0.282)[d]	6.8 (±0.282)[c]
Group 5 (C-Ag NPs)	33.16 (±0.226)[e]	0.098 (±0.495)[c]	22.115 (±0.161)[d]	3.2 (±0.141)[e]	4.2 (±0.3)[e]
Group 6 (C-Ag@nGO NCs)	23.62 (±0.544)[f]	0.075 (±0.005)[c]	26.125 (±0.176)[e]	2.05 (±0.07)[f]	2.6 (±0.8)[f]

nGO Nano-graphene oxide, *B-Ag NPs* Biogenic silver nanoparticles, *B-Ag@nGO NCs* Biogenic silver nano-graphene oxide nanocomposites, *C-Ag NPs* Chemical silver nanoparticles, *C-Ag@nGO NCs* Chemical silver nano-graphene oxide nanocomposites

**Different superscript letters (a,b,…,f) indicate statistical differences

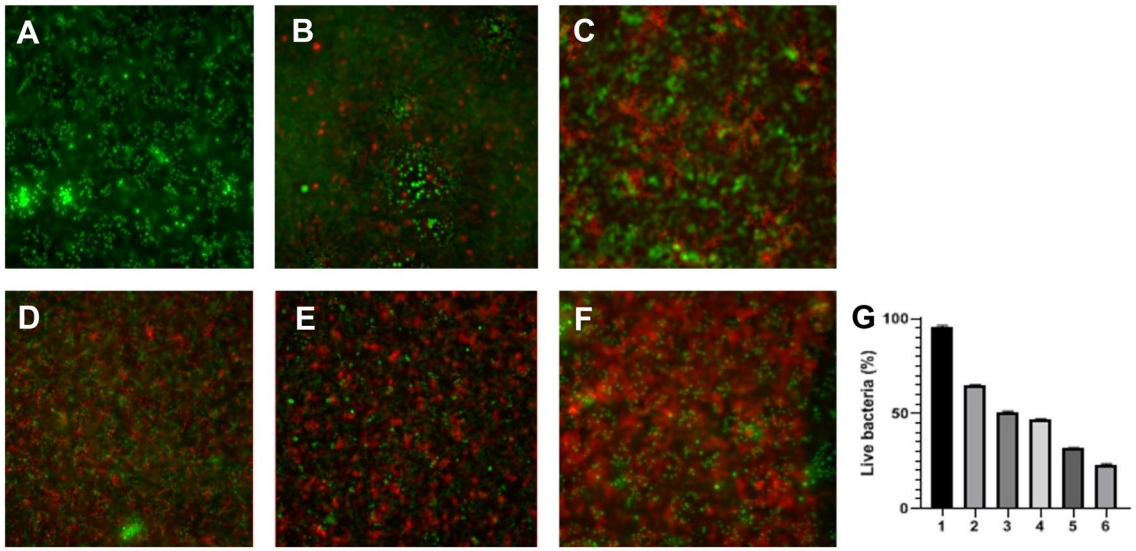

Fig. 5 Confocal microscope images of groups: **A** Control **B** nGO **C** B-Ag NPs **D** B-Ag@nGO NCs **E** C-Ag NPs **F** C-Ag@nGO NCs **G** Live bacteria (%), Group 1: Control, Group 2: nGO, Group 3: B-Ag NPs, Group 4: B-Ag@nGO NCs, Group 5: C-Ag NPs, Group 6: C-Ag@nGO NCs. (*nGO* nano-graphene oxide, *B-Ag NPs* Biogenic silver nanoparticles, *B-Ag@nGO NCs* Biogenic silver nano-graphene oxide nanocomposites, *C-Ag NPs* Chemical silver nanoparticles, *C-Ag@nGO NCs* Chemical silver nano-graphene oxide nanocomposites)

with the control group. According to these results, the null hypothesis of our study was partially accepted.

Ag NPs are frequently used in various fields and dentistry due to their antibacterial properties. The antibacterial mechanism of Ag NPs is that Ag ions cause cell death by activating the enzymes of bacteria [40]. In studies, Ag NPs have been added to many dental materials such as dental composites, dental adhesives, and glass ionomer cement, and their antibacterial activity has been proved [13, 41–43]. Ag NPs impart antibacterial, antifungal, and antiviral activity to dental resins [44]. Therefore, Ag NPs were preferred as antibacterial nanoparticles in our study.

A small amount of Ag NPs should be used so that it does not adversely affect the color, aesthetics, and mechanical properties of dental materials [13]. The results of the studies showed that Ag NPs, used in appropriate proportions, impart a strong antibacterial activity that greatly reduces biofilm growth and lactic acid production without adversely affecting other physical and mechanical properties of the resins [10–13]. In studies, the amount of Ag NPs in the dental adhesive is generally 0.05% and 0.1% by weight [35, 45]. It is aimed to obtain the highest efficiency at the lowest concentration from Ag NP used in materials expected to be developed with nanotechnological approaches Ag NPs of different weights (0.25%, 0.05%, 0.1%) were tested in our study. When 0.05% by weight of NPs was used, it provided a similar antibacterial activity to 0.1% by weight. For this reason, 0.05% Ag NPs were

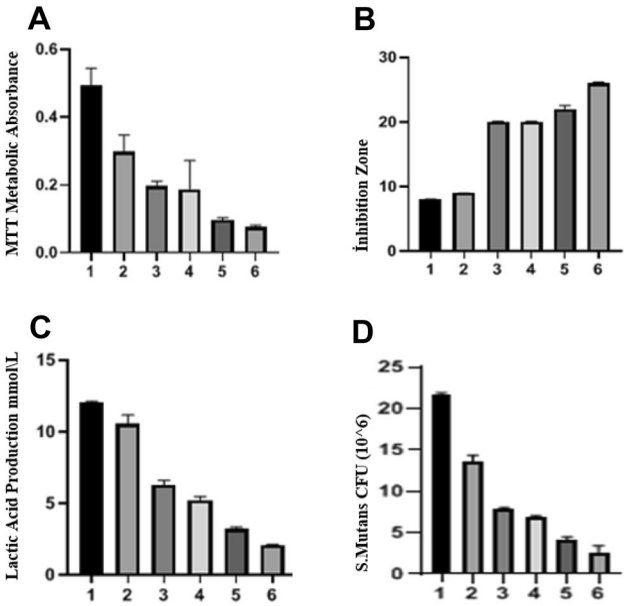

Fig. 6 **A** MTT metabolic activity, **B** Zone of inhibition (mm), **C** Lactic acid production (mmol/L), **D** *S. mutans* colony-forming unit (CFU), Group 1: Control, Group 2: nGO, Group 3: B-Ag NPs, Group 4: B-Ag@nGO NCs, Group 5: C-Ag NPs, Group 6: C-Ag@nGO NCs. (*nGO* nano-graphene oxide, *B-Ag NPs* Biogenic silver nanoparticles, *B-Ag@nGO NCs* Biogenic silver nano-graphene oxide nanocomposites, *C-Ag NPs* Chemical silver nanoparticles, *C-Ag@nGO NCs* Chemical silver nano-graphene oxide nanocomposites)

used in our study to eliminate the negative effects of high concentrations.

Although different kinds of plant extracts are used to obtain green synthesis NPs, the reason why we prefer Chamomile extract for Ag NPs synthesis is that it is biocompatible, acts as a good reducing agent, and has antibacterial and antioxidant activity [28, 46].

Studies have shown that Ag NPs fixed on the nGO surface have greater antibacterial activity [29–31]. Therefore, in our study, Ag NPs synthesized by green and chemical methods to increase the antibacterial activity of Ag NPs were fixed on nGO to obtain Ag@nGO NCs and added to the dental adhesive. According to the results of our study, both C–Ag@nGO and B-Ag@nGO NCs exhibited a much more effective antimicrobial activity compared to individual C–Ag and B-Ag NPs. Akram et al. [47] in their study, they added 0.25–0.5% reduced nano-graphene oxide (RGO) doped with silver nanoparticles (nAg) (RGO/nAg) and 0.25–0.5% graphene nanoplatelets (GNPs) doped with nAg (GNP/nAg) into the dental adhesive (Scotchbond™ Universal adhesive, 3 M ESPE, St. Paul, MN, USA). In the study, resin-dentin bonded interface were investigated by evaluating interfacial nanoleakage, micropermeability, nanodynamic mechanical analysis, μTBS. As a result of the study, 0.25% GNP/nAg showed sufficient anti-biofilm properties without affecting the dentin bond strength properties.In another study, it was shown that the incorporation of Ag@GO NCs into conventional glass ionomer cement (CIS) significantly inhibited the growth of *S. mutans* in vitro. Ag@GO NCs, added to the glass ionomer cement at a concentration of about 2% by weight, provided antibacterial properties without compromising the mechanical performance of the glass ionomer cement [29]. In the study by Wu et al. [31], the inhibitory effect of Ag@GO NCs on artificial enamel lesions was investigated. According to the results of the study, Ag@GO NCs groups compared to the control groups; ıt decreased enamel surface roughness, shallow lesion depth, and a decrease in mineral loss. In another study, Ag@GO NCs were used as an endodontic irrigation solution and had higher antibacterial and antibiofilm capacity compared to the control group [48]. The reason is that the Ag NPs decorated GO may wrap the surface of target bacterial cells and interact with almost the whole cell surface, which induces rapid cell membrane deformation and eventual cell death. The other reason for these results is that GO, which is used as a platform to fix nanoparticles and prevent aggregation, provides a more antibacterial activity by increasing the dispersion of Ag NPs.

In our study, the lowest S. mutans survival rate, lactic acid production, and colony count were observed in the group containing C–Ag@nGO NCs. In millimeters, the largest

Table 2 The distribution of bond strength values, standard deviations, and failure modes of groups

Groups ($n=20$)	Bond strength (MPa)			FailureModes [n (%)]		
	Mean ± SD	Min	Max	Adhesive	Cohesive	Mixed
Group 1 (Control)	18.51 (±2.48)[a]	13.5	22.1	0 (%0)	2 (%10)	18 (%90)
Group 2 (nGO)	18.46 (±2.42)[a]	12.2	22.5	5 (%25)	5 (%25)	10 (%50)
Group 3 (B-Ag NPs)	18.59 (±2.62)[a]	14.4	23.1	3 (%15)	5 (%25)	12 (%60)
Group 4 (B-Ag@nGO NCs)	18.23 (±2.47)[a]	14.7	24.1	5 (%25)	6 (%30)	9 (%45)
Group 5 (C-Ag NPs)	18.34 (±2.07)[a]	13.8	23.3	1 (%5)	15 (%75)	4 (%20)
Group 6 (C-Ag@nGO NCs)	17.97 (±2.12)[a]	12.5	21.9	1 (%5)	11 (%55)	8 (%40)

B-Ag NPs Biogenic silver nanoparticles, *B-Ag@nGO NCs* Biogenic silver nano-graphene oxide nanocomposites, *C-Ag NPs* Chemical silver nanoparticles, *C-Ag@nGO NCs* Chemical silver nano-graphene oxide nanocomposites

inhibition zone was seen in the group containing C–Ag@nGO NCs. The reason why the antibacterial activity of the groups containing C–Ag NPs/Ag@nGO NCs was higher than the group containing the B-Ag NPs/Ag@nGO NCs may be related to the synthesis method. The advantage of this method is that nanoparticles can be synthesized in the desired size and shape by chemical synthesis and the molecular stability of the obtained nanoparticles is good [49–51]. However, the biggest disadvantage of the chemical synthesis method is the toxicity of the reducing agents used in the synthesis. Green synthesis has advantages such as being biocompatible and being able to be synthesized in large quantities at low cost. However, besides these advantages, the contents of the plants used in green synthesis reactions; can slow down the reaction, decrease the stability of Ag NPs and cause aggregation [29, 46]. Additionally, another disadvantage of the green synthesis method is that it is difficult to control the size and shape of nanoparticles [28]. This may be the reason why the antibacterial activity is lower in B-Ag NPs/Ag@nGO NCs groups compared to C–Ag NPs/Ag@nGO NCs groups.

Although the antibacterial activity of Ag NPs obtained by green synthesis is lower than that of chemically synthesis-obtained Ag NPs, they provided higher antibacterial activity compared to the control group. Kulshrestha et al. [52] synthesized Ag@nGO NCs by the green synthesis method using persian flower extract from Legistromia speciosa in a study they conducted and evaluated its antibacterial activity. Similar to our study, in this study, Ag@nGO NCs reduced biofilm formation in both Gram-negative (*E. cloacae*) and Gram-positive (*S. mutans*) bacterial models.

Bond strength tests were used to evaluate the bonding ability of restorative materials to enamel and dentine. Shear and tensile test methods are the most frequently preferred bond strength tests for this purpose (Table 2). Studies have reported that the μTBS test method is one of the appropriate and safe test methods in testing the bond strength of adhesive materials to dentine [2, 33, 53]. Similar to previous studies, the μTBS test was preferred to evaluate the bond strength of the experimental adhesives formed in our study to dentine [2, 33]. According to our study results, there was no statistical difference between the groups in the μTBS test results. Nanoparticles added to the adhesive resin did not reduce the adhesion force. In a similar study, Ag NPs were added to Scotchbond Multi-Purpose adhesive resin (SBMP) at different concentrations (50, 100, 150, 200, and 250 ppm). According to the results of the study, 200 and 250 ppm Ag NPs containing groups had similar μTBS to the control group [2]. In another study, 0.05% by mass of Ag NPs were added into Scotchbond Multi-Purpose adhesive resin (SBMP). Ag NPs added group showed similar μTBS compared to the control group [33]. The results of our study on groups containing Ag NPs are compatible with these studies. Akram et al. [47] in their result of the study, 0.25% GNP/nAg showed sufficient anti-biofilm properties without affecting the dentin bond strength properties. However, in this study, chemical synthesis method was used instead of biosynthetic green synthesis method in NP production. The difference of our study is that the Ag NP and Ag@nGO NCs used were produced by the green synthesis method using chamomile plant and two-stage adhesive was used.

In our study, when the failure modes after the μTBS test were evaluated, the most common type of failure observed was a mixed mode, followed by cohesive mode failure, and the least common type of failure was adhesive mode. It has been reported that the mixed failure mode is mostly seen at interfaces where the stress distribution is not homogeneous [54]. The low number of adhesive failure modes can be interpreted as strong adhesive bonding in the control and experimental groups. There are studies in the literature reporting that there is no correlation between bond strength and failure modes [55, 56]. In our study, when the bond strength values and failure modes of the groups were compared, it was seen that there was no correlation between these two parameters.

The strength of our study is that Ag NPs and Ag@nGO NCs produced by the green synthesis method were used in dental adhesive for the first time. Ag NPs and Ag@nGO NCs provided antibacterial activity without affecting bond strength. These results will guide the use of NPs and GO produced by the green synthesis method to provide antibacterial activity to dental materials in future studies. The limitations of this study are that the in vitro conditions did not fully meet the oral conditions, and the biocompatibility and cytotoxicity of the materials were not evaluated. Additionally, the time-dependent change in the antibacterial effect and mechanical properties have not been tested. Further in vitro and in vivo studies must confirm the study results.

Conclusion

According to the results obtained within the limitations of this study, adhesive groups containing C–Ag NPs and C–Ag@nGO NCs showed higher antibacterial activity than groups of B-Ag NPs and B-Ag@nGO NCs. Adhesive groups containing B-Ag NPs and B-Ag@nGO NCs showed higher antibacterial activity than the control group. According to our results, nGO can be used in dental materials to increase the dispersion and antibacterial activity of Ag NPs. Additionally, since there is no difference between the groups in terms of dentin bond strength values, nanoparticles obtained by the green synthesis method can be preferred to eliminate the disadvantages of the chemical synthesis method. Further studies are needed to obtain more detailed results on this subject.

Funding This study was funded by the Technological and Scientific Council of Turkey (TUBITAK) (Project number: 220S445).

Declarations

Conflict of interest The authors declare that they have no known competing financial interests or personal relation ships that could have appeared influence the work reported in this paper.

Ethical approval This study protocol was approved by the Erciyes University Faculty of Medicine Ethics Committee (2020/519).

References

1. Mjor IA, Toffenetti F. Secondary caries: a literature review with case reports. Quintessence Int. 2000;31:165–79.
2. Amin F, Fareed MA, Zafar MS, Khurshid Z, Palma PJ, Kumar N. Degradation and stabilization of resin-dentine interfaces in polymeric dental adhesives: an updated review. Coatings. 2022;12:1094. https://doi.org/10.3390/coatings12081094.
3. Dutra-Correa M, Leite A. Antibacterial effects and cytotoxicity of an adhesive containing low concentration of silver nanoparticles. J Dent. 2018;77:66–71. https://doi.org/10.1016/j.jdent.2018.07.010.
4. Fruits TJ, Knapp JA, Khajotia SS. Microleakage in the proximal walls of direct and indirect posterior resin slot restorations. Oper Dent. 2006;31:719–27. https://doi.org/10.2341/05-148.
5. Tavassoli HS, Alaghemand H, Hamze F. Antibacterial, physical and mechanical properties of flowable resin composites containing zinc oxide nanoparticles. Dent Mater. 2013;29:495–505. https://doi.org/10.1016/j.dental.2013.03.011.
6. Mansoor A, Khurshid Z, Khan MT, Mansoor E, Butt FA, Jamal A, Palma PJ. Medical and dental applications of titania nanoparticles: an overview. Nanomaterials. 2022;12:3670. https://doi.org/10.3390/nano12203670.
7. Choi O, Deng KK, Kim NJ, Ross L, Surampalli RY, Hu Z. The inhibitory effects of silver nanoparticles, silver ions, and silver chloride colloids on microbial growth. Water Res. 2008;42:3066–74. https://doi.org/10.1016/j.watres.2008.02.021.
8. Ocsoy I, Paret ML, Ocsoy MA, Kunwar S, Chen T, You M, Tan W. Nanotechnology in plant disease management: DNA-directed silver nanoparticles on graphene oxide as an antibacterial against *Xanthomonas perforans*. ACS Nano. 2013;7:8972–80. https://doi.org/10.1021/nn4034794.
9. Ocsoy I, Gulbakan B, Chen T, Zhu G, Chen Z, Sari MM. Tan W DNA-guided metal-nanoparticle formation on graphene oxide surface. Adv Mater. 2013;25:2319–25. https://doi.org/10.1002/adma.201204944.
10. Ahn SJ, Lee SJ, Kook JK, Lim BS. Experimental antimicrobial orthodontic adhesives using nanofillers and silver nanoparticles. Dent Mater. 2009;25:206–13. https://doi.org/10.1016/j.dental.2008.06.002.
11. Besinis A, De Peralta T, Handy RD. Inhibition of biofilm formation and antibacterial properties of a silver nanocoating on human dentine. Nanotoxicology. 2014;8:745–54. https://doi.org/10.3109/17435390.2013.825343.
12. Cheng YJ, Zeiger DN, Howarter JA, Zhang X, Lin NJ, Antonucci MJ, Lin-Gibson S. In situ formation of silver nanoparticles in photocrosslinking polymers. J Biomed Mater Res B Appl Biomater. 2011;97:124–31. https://doi.org/10.1002/jbm.b.31793.
13. Fan C, Chu L, Rawls HR, Norling BK, Cardenas HL, Whang K. Development of an antimicrobial resin-a pilot study. Dent Mater. 2011;27:322–8. https://doi.org/10.1016/j.dental.2010.11.008.
14. Duarte SJ, Lolato AL, Freitas CR, Dinelli W. SEM analysis of internal adaptation of adhesive restorations after contamination with saliva. J Adhes Dent. 2005;7:51–6.
15. Lynch CD, Frazier KB, Mcconnell RJ, Blum IR, Wilson NH. Minimally invasive management of dental caries: contemporary teaching of posterior resin-based composite placement in U.S. and Canadian dental schools. J Am Dent Assoc. 2011;142:612–20. https://doi.org/10.14219/jada.archive.2011.0243.
16. Imazato S, Kuramoto A, Takahashi Y, Ebisu S, Peters MC. In vitro antibacterial effects of the dentine primer of Clearfil Protect Bond. Dent Mater. 2006;22:527–32. https://doi.org/10.1016/j.dental.2005.05.009.
17. Karatoprak GŞ, Aydin G, Altinsoy B, Altinkaynak C, Koşar M, Ocsoy I. The effect of *Pelargonium endlicherianum* Fenzl. root extracts on formation of nanoparticles and their antimicrobial activities. Enzyme Microb Technol. 2017;97:21–6. https://doi.org/10.1016/j.enzmictec.2016.10.019.
18. Ocsoy I, Tasdemir D, Mazicioglu S, Celik C, Katı A, Ulgen F. Biomolecules incorporated metallic nanoparticles synthesis and their biomedical applications. Mater Lett. 2018;212:45–50. https://doi.org/10.1016/j.matlet.2017.10.068.
19. Ocsoy I, Temiz M, Celik C, Altinsoy B, Yilmaz V, Duman F. A green approach for formation of silver nanoparticles on magnetic graphene oxide and highly effective antimicrobial activity and reusability. J Mol Liq. 2017;227:147–52. https://doi.org/10.1016/j.molliq.2016.12.015.
20. Strayer A, Ocsoy I, Tan W, Jones JB, Paret ML. Low concentrations of a silver-based nanocomposite to manage bacterial spot of tomato in the greenhouse. Plant Dis. 2016;100:1460–5. https://doi.org/10.1094/PDIS-05-15-0580-RE.
21. Dogru E, Demirbas A, Altinsoy B, Duman F, Ocsoy I. Formation of Matricaria chamomilla extract-incorporated Ag nanoparticles and size-dependent enhanced antimicrobial property. J Photochem Photobiol B. 2017;174:78–83. https://doi.org/10.1016/j.jphotobiol.2017.07.024.
22. Ocsoy I, Demirbas A, McLamore ES, Altinsoy B, Ildiz N, Baldemir A. Green synthesis with incorporated hydrothermal approaches for silver nanoparticles formation and enhanced antimicrobial activity against bacterial and fungal pathogens. J Mol Liq. 2017;238:263–9. https://doi.org/10.1016/j.molliq.2017.05.012.
23. Ekrikaya S, Yilmaz E, Celik C, Demirbuga S, Ildiz N, Demirbas A, Ocsoy I. Investigation of ellagic acid rich-berry extracts directed silver nanoparticles synthesis and their antimicrobial properties with potential mechanisms towards *Enterococcus faecalis* and *Candida albicans*. J Biotechnol. 2021;341:155–62. https://doi.org/10.1016/j.jbiotec.2021.09.020.
24. Some S, Bulut O, Biswas K, Kumar A, Roy A, Sen IK, Ocsoy I. Effect of feed supplementation with biosynthesized silver nanoparticles using leaf extract of *Morus indica* L. V1 on *Bombyx mori* L. (Lepidoptera: Bombycidae). Sci Rep. 2019;9:1–13. https://doi.org/10.1038/s41598-019-50906-6.
25. Some S, Sen IK, Mandal A, Aslan T, Ustun Y, Yilmaz EŞ, Ocsoy I. Biosynthesis of silver nanoparticles and their versatile antimicrobial properties. Mater Res Express. 2018;6:012001. https://doi.org/10.1088/2053-1591/aae23e.
26. Altinsoy BD, Karatoprak GŞ, Ocsoy I. Extracellular directed ag NPs formation and investigation of their antimicrobial and cytotoxic properties. Saudi Pharm J. 2019;27:9–16. https://doi.org/10.1016/j.jsps.2018.07.013.
27. Demirbas A, Yilmaz V, Ildiz N, Baldemir A, Ocsoy I. Anthocyanins-rich berry extracts directed formation of Ag NPs with the investigation of their antioxidant and antimicrobial activities. J

Mol Liq. 2017;248:1044–9. https://doi.org/10.1016/j.molliq.2017.10.130.
28. Skandalis N, Dimopoulou A, Georgopoulou A, Gallios N, Papadopoulos D, Tsipas D. The effect of silver nanoparticles size, produced using plant extract from *Arbutus unedo*, on their antibacterial efficacy. Nanomaterials. 2017;7:178–92. https://doi.org/10.3390/nano7070178.
29. Jingwen C, Zhaob Q, Penga J, Yanga X, Yua D, Zhaoa W. Antibacterial and mechanical properties of reduced graphene-silver nanoparticle nanocomposite modified glass ionomer cements. Dent Mater. 2020;96:103332. https://doi.org/10.1016/j.jdent.2020.103332.
30. Nizami MZI, Takashiba S, Nishina Y. Graphene oxide: a new direction in dentistry. Appl Mater Today. 2020;19:100576. https://doi.org/10.1016/j.apmt.2020.100576.
31. Wu R, Zhao Q, Lu S, Fu Y, Yu D, Zhao W. Inhibitory effect of reduced graphene oxide-silver nanocomposite on progression of artificial enamel caries. J Appl Oral Sci. 2018;27:20180042. https://doi.org/10.1590/1678-7757-2018-0042.
32. Song B, Zhang C, Zeng G, Gong J, Chang Y. Antibacterial properties and mechanism of graphene oxide-silver nanocomposites as bactericidal agents for water disinfection. Arch Biochem Biophys. 2019;604:1–10. https://doi.org/10.1016/j.abb.2016.04.018.
33. Li F, Weir MD, Chen J. Xu HH Comparison of quaternary ammonium-containing with nano-silver-containing adhesive in antibacterial properties and cytotoxicity. Dent Mater. 2013;29:450–61. https://doi.org/10.1016/j.dental.2013.01.012.
34. Cheng L, Exterkate RA, Zhou X, Li J, ten Cate JM. Effect of *Galla chinensis* on growth and metabolism of microcosm biofilms. Caries Res. 2011;45:87–92. https://doi.org/10.1159/000324084.
35. Li F, Weir MD, Fouad AF, Xu HHK. Effect of salivary pellicle on antibacterial activity of novel antibacterial dental adhesives using a dental plaque microcosm biofilm model. Dent Mater. 2014;30:182–91. https://doi.org/10.1016/j.dental.2013.11.004.
36. Zhang K, Cheng L, Imazato S. Effects of dual antibacterial agents MDPB and nano-silver in primer on microcosm biofilm, cytotoxicity and dentine bond properties. J Dent. 2013;41:464–74. https://doi.org/10.1016/j.jdent.2013.02.001.
37. Cheng L, Weir MD, Xu HHK, Antonucci JM, Kraigsley AM, Lin NJ, et al. Antibacterial amorphous calcium phosphate nanocomposite with quaternary ammonium salt and silver nanoparticles. Dent Mater. 2012;28:561–72. https://doi.org/10.1016/j.dental.2012.01.005.
38. Cheng L, Zhang K, Melo MAS, Weir MD, Zhou XD, Xu HHK. Anti-biofilm dentin primer with quaternary ammonium and silver nanoparticles. J Dent Res. 2012;91:598–604. https://doi.org/10.1177/00220345124441.
39. Perdigao J, Swift E, Walter R. Fundamental concepts of enamel and dentin adhesion. In: Roberson TM, Heyman HO, Swift E. Sturdevant's Art and Science of operative dentistry. St. Louis: Mosby Elsevier 2014;6:114-140.
40. Rai M, Yadav A, Gade A. Silver nanoparticles as a new generation of antimicrobials. Biotechnol Adv. 2009;27:76–83. https://doi.org/10.1016/j.biotechadv.2008.09.002.
41. Lu Z, Rong K, Li J, Yang H, Chen R. Size dependent antibacterial activities of silver nanoparticles against oral anaerobic pathogenic bacteria. J Mater Sci Mater Med. 2013;24:1465–71. https://doi.org/10.1007/s10856-013-4894-5.
42. Jandt KD, Watts DC. Nanotechnology in dentistry: Present and future perspectives on dental nanomaterials. Dent Mater. 2020;36:1365–678. https://doi.org/10.1016/j.dental.2020.08.006.
43. Porter G, Tompkins G, Schwass D, Li K, Waddell J, Meledandri C. Anti-biofilm activity of silver nanoparticle-containing glass ionomer cements. Dent Mater. 2020;36:1096–107. https://doi.org/10.1016/j.dental.2020.05.001.
44. Monteiro DR, Gorup LF, Takamiya AS, Ruvollo-Filho AC, Camargo ER, Barbosa DB. The growing importance of materials that prevent microbial adhesion: antimicrobial effect of medical devices containing silver. Int J Antimicrob. 2009;34:103–10. https://doi.org/10.1016/j.ijantimicag.2009.01.017.
45. Melo MA, Cheng L, Zhang K, Weir MD, Rodrigues LK, Xu HH. Novel dental adhesives containing nanoparticles of silver and amorphous calcium phosphate. Dent Mater. 2013;29:199–210. https://doi.org/10.1016/j.dental.2012.10.005.
46. Duman F, Ocsoy I, Kup FO. Chamomile flower extract-directed CuO nanoparticle formation for its antioxidant and DNA cleavage properties. Mater Sci Eng C. 2016;60:333–8. https://doi.org/10.1016/j.msec.2015.11.052.
47. Akram Z, Aati S, Clode P, Saunders M, Ngo H, Fawzy AS. Formulation of nano-graphene doped with nano silver modified dentin bonding agents with enhanced interfacial stability and antibiofilm properties. Dent Mater. 2022;38:347–62. https://doi.org/10.1016/j.dental.2021.12.016.
48. Ioannidis K, Niazi S, Mylonas P, Mannocci F, Deb S. The synthesis of nano silver-graphene oxide system and its efficacy against endodontic biofilms using a novel tooth model. Dent Mater. 2019;35:1614–929. https://doi.org/10.1016/j.dental.2019.08.105.
49. El Badawy AM, et al. Surface charge-dependent toxicity of silver nanoparticles. Environ Sci Technol. 2011;45:283–7. https://doi.org/10.1021/es1034188.
50. Sileikaite A, Puiso J, Prosycevas I, Tamulevicius S. Investigation of silver nanoparticles formation kinetics during reduction of silver nitrate with sodium citrate. Mater Sci. 2009;15:21–7.
51. Iravani S, Korbekandi H, Mirmohammadi SV, Zolfaghari B. Synthesis of silver nanoparticles: chemical, physical and biological methods. Res Pharm Sci. 2004;9:385.
52. Kulshrestha S, Qayyum S, Khan AU. Antibiofilm efficacy of green synthesized graphene oxide-silver nanocomposite using *Lagerstroemia speciosa* floral extract: a comparative study on inhibition of gram-positive and gram-negative biofilms. Microb Pathog. 2017;103:167–77. https://doi.org/10.1016/j.micpath.2016.12.022.
53. Salz U, Bock T. Testing adhesion of direct restoratives to dental hard tissue-a review. J Adhes Dent. 2019;12:343–71. https://doi.org/10.3290/j.jad.a19741.
54. Moule CA, Angelis F, Kim GH, Le S, Malipatil S, Foo MS, Burrow MF, Thomas D. Resin bonding using an all-etch or self-etch adhesive to enamel after carbamide peroxide and/or CPP-ACP treatment. Aust Dent J. 2007;52:133–7. https://doi.org/10.1111/j.1834-7819.2007.tb00478.x.
55. El-din AN, Miller B, Griggs J, Wakefield C. Immediate bonding to bleached enamel. Oper Dent. 2006;31:106–14. https://doi.org/10.2341/04-201.
56. Gurgan S, Alpaslan T, Kiremitci A, Cakir FY, Yazıcı E, Gorucu J. Effect of different adhesive systems and laser treatment on the shear bond strength of bleached enamel. J Dent. 2009;37:527–34. https://doi.org/10.1016/j.jdent.2009.03.012.

Publisher's Note Springer Nature remains neutral with regard to jurisdictional claims in published maps and institutional affiliations.

Springer Nature or its licensor (e.g. a society or other partner) holds exclusive rights to this article under a publishing agreement with the author(s) or other rightsholder(s); author self-archiving of the accepted manuscript version of this article is solely governed by the terms of such publishing agreement and applicable law.